PHYSOR 2004 -The Physics of Fuel Cycles and Advanced Nuclear Systems: Global Developments
Chicago, Illinois, April 25-29, 2004, on CD-ROM, American Nuclear Society, Lagrange Park, IL. (2004)

Assessment of CASMO-4 Predictions of the Isotopic Inventory of High Burn-Up MOX Fuel

Rafael Macian[*1], Martin A. Zimmermann[1] and Rakesh Chawla[1,2]
[1]*Paul Scherrer Institute, Villigen PSI, CH-5232 Switzerland*
[2]*Swiss Federal Institute of Technology (EPFL), Lausanne, Switzerland*

The current paper presents an assessment of the depletion model in CASMO-4 based on highly-burnt MOX fuel data from the Programme ARIANE. Isotopic compositions calculated with CASMO-4 for a sample irradiated for 6 cycles in the Swiss PWR Beznau-1 have been compared with experimental data from the PSI and SCK•CEN radio-chemical laboratories. Both a 1-D pin-cell and a 2-D fuel-assembly model have been used, together with detailed and burn-up averaged irradiation histories. The results obtained (a) show that predictions for the most important actinides have errors below 10%, (b) highlight problems with Am and Eu isotopes, and (c) indicate experimental inaccuracies probably linked to the measurement techniques for ^{129}I and some metallic fission products. Additional studies, focused on refined pin-cell treatment, have found that such modeling effects can be significant for the prediction of some actinides, e.g. Pu, Cm and Am.

KEYWORDS: CASMO-4, MOX, ARIANE, high burn-up, fuel isotopics

1. Introduction

The accurate calculation of isotopic content is of great importance for a number of reactor physics applications, e.g. computation of precise macroscopic cross section data for criticality and burn-up credit calculations, as well as for fuel cycle back-end considerations such as radiotoxicity evaluations. In order to provide the nuclear community with an experimental data base containing a large number of accurately measured isotope inventories (some of them in very low concentration) from different kinds of irradiated fuels, the ARIANE (Actinides Research In A Nuclear Element) Programme [1,2] was started in 1994. Irradiated fuel samples from several light-water reactors, including the Swiss Gösgen and Beznau PWRs (UO2 and mixed uranium-plutonium oxide (MOX) fuel samples, respectively) and the Dutch Dodewaard BWR (both UO2 and MOX), were analyzed radio-chemically by three nuclear centers, namely SCK•CEN (Belgium), PSI (Switzerland) and ITU (Germany), using different analytical methods. The final report with the sample compositions was issued in December 2000 [2]. CASMO-4 [3,4] is one of the most widely used production codes employed for LWR 2D-assembly calculations in the framework of both core-design and core-follow work. This makes the assessment of the accuracy of its depletion methodology particularly important, especially for its application to the analysis of high burn-up fuel. Also, a relatively large number of light water reactors in Europe currently operate with MOX fuel in their cores and, by 2010, 16 to 18 reactors are expected to burn MOX in Japan. Therefore, it is clear that the accurate prediction of irradiated MOX fuel isotopics is important for fuel assembly design, core physics analysis, and a variety of reactor safety and licensing applications.

[*] Corresponding author, Tel. +41-56-310-2701, FAX +41-56-310-2327, E-mail: rafael.macian@psi.ch

For these reasons, the isotopic inventories of the highly irradiated MOX fuel samples from the ARIANE Programme are particularly valuable for assessing the accuracy of the CASMO-4 burn-up methodology. The current paper presents, in this context, the results obtained for one of the PWR fuel samples.

2. The Depletion Model in CASMO-4

The depletion model in CASMO-4 solves the coupled non-linear system of depletion equations in Eq. (1) [3]:

$$\frac{d\,N_m(t)}{dt} = \left[\; Production\ Rate - Removal\ Rate - Total\ Fission\ Yield \;\right]_m \quad m = 1 \ldots n\ Nuclides \tag{1}$$

The removal term includes losses by radioactive decay and neutron absorption, a function of the microscopic cross-section and neutron flux for each energy group. The production rate term considers all the main paths through which a nuclide can appear in the fuel, i.e. radioactive decay of other nuclides and neutron-capture reactions of predecessors. The total fission yield term for nuclide *m* is based on the integrated number of fissions for each nuclide that produces nuclide *m*. Nuclide production reaction rates also include branching ratios from the neutronic data libraries. CASMO-4 uses a two-step "predictor-corrector" numerical scheme to solve Eq.(1), which permits the use of relatively large burn-up intervals, while maintaining the accuracy of the results.

3. Description of the Fuel Sample

The well-characterized MOX sample analyzed in the study described in this paper belonged to a segmented MOX fuel rod, K7, in the Belgonucleaire fuel assembly M308 irradiated for 6 cycles (20 to 25) in Beznau-1.

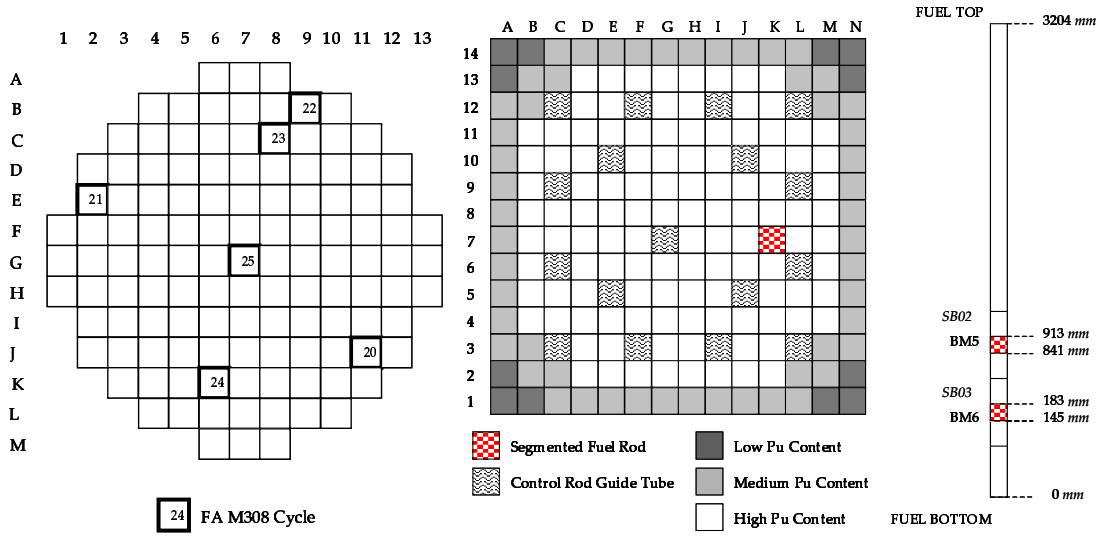

Fig. 1 Location of Fuel Assembly M308 during Irradiation, of Fuel Rod K7 in Assembly M308, and of Sample BM5 in Rod K7

Fuel assembly M308 was shuffled in the core during re-loading outages; its different locations are shown on the left in Figure 1. The total average rod burn-up was calculated to be

52 MWd/kgMH, with a pellet peak burn-up of 59 MWd/kgHM. M308 was a 14x14 PWR assembly with 179 fuel rods arranged in three MOX enrichment zones (4.12, 2.91, and 2.29 *w/o Pu with respect to heavy metal*). These are depicted in the central part of Figure 2 in three different shades, with the Rod K7 position indicated as checkered square, viz. in the high PuO_2 content zone near a water-filled guide tube (L6). Sample BM5 (5.5 *w/o* Pu with respect to heavy metal) located 841 to 913 mm from bottom in the largest axial power peak region of Rod K7, as indicated in Figure 2 (*right*), had a calculated [1] discharge burn-up of 58.9 MWd/kgMH.

4. CASMO-4 Fuel Depletion Model

4.1 Sample Model

As mentioned above, both a simplified 1-D pin-cell description of the fuel assembly and a 2-D fuel-assembly model were used. Comparison of the results for these two models allowed the analysis of the effect of the intra-assembly neutron flux distribution on fission product build-up and fuel burn-up. In defining the equivalent cell, spectral effects of the surrounding fuel pins and of guide tubes and metallic structures were accounted for by means of an appropriate homogenization technique that added a certain content of Zr to the moderator region of the pin-cell with an equivalent radius, r_{eq}, calculated from the equivalent rod pitch, p_{eq} (see Figure 2).

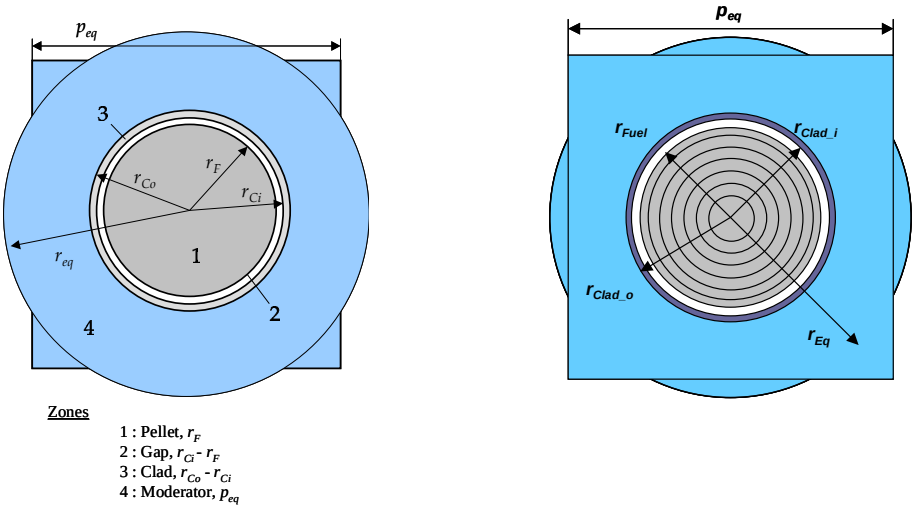

Fig. 2 CASMO-4 Pin-Cell Model for Sample BM5 Base Case (1 Fuel Zone; *right*) and Refined Pin-Cell (7 Fuel Zones; *left*)

The power density input value is directly assigned by CASMO-4 to the only fuel region that constitutes the pin-cell model. In the fuel assembly model, this value is an *average* for the sample axial plane. The CASMO-4 solution determines the pin power density for the depletion of the sample, which may not *exactly* coincide with the value given by the depletion history. The power density influences the nuclide build-up through the calculation of the power average normalization factor in the depletion equations. Seven and ten fuel-pellet radial zones were used in the 1-D and 2-D models, respectively (maximum allowed by CASMO-4), in order to resolve the effects of the intra-pellet neutron flux and spectrum on the build-up of important actinides, viz. Pu, U, Cm, Am, etc.

4.2 Irradiation History

Reference [1] contains the detailed (6-cycle) irradiation history of Sample BM5 as calculated by Belgonucleaire. The data include moderator temperature, moderator density, boron content, fuel temperature, and power density at the sample location, as a function of burn-up. Based on this information, calculations were carried out with CASMO-4 which modeled the detailed irradiation history, a cycle-averaged history, and a full six-cycle averaged history, with averaging based on the burn-up step length. All the calculations assumed that the conditions changed at the end of each depletion step, and stayed constant throughout the step. The power density for the sample was calculated from the data for the assembly-average power density in Ref.[2] and the axial peaking factor at the sample location obtained from a SIMULATE-3 core-follow calculation with Beznau-1 plant data.

4.3 Libraries

Two neutron data libraries were used for the depletion study, viz. a standard library based on data from ENDF/B-IV (complemented with additional data from other sources for 108 materials) and the J2LIB neutron data library. Neutronic data in the ENDF/B-IV library are tabulated for 70 energy groups and structured as in the WIMS code with an additional boundary at 1.855 eV. The 0.3 eV and 1 eV resonances of ^{239}Pu and ^{240}Pu, respectively, are adequately taken into account by the WIMS structure. The fission spectra for ^{235}U and ^{239}Pu are taken from ENDFB-V, and data for ^{241}Pu from JENDL-2.

The J2LIB neutronic data library used by CASMO-4 is based on the JEF-2.2 evaluated data file developed at the OECD/NEA data bank, and processed with NJOY-91.91. It provides data for a larger number of nuclides than the code's ENDF/B-IV based library and the cross-sections are tabulated in 70 groups with a similar structure as that of the ENDF/B-IV based library.

4.4 Calculation Procedure

CASMO-4 input files containing all the necessary information for the depletion of the MOX samples, i.e. model geometric parameters, initial isotopic inventory from Ref.[1, 2], and the data on the irradiation histories, were developed for each case according to the recommendations in Ref.[1]. The calculations proceeded up to the point of interest in the Sample BM5 depletion history. Thus, for the pin-cell calculations, the power burn-up stopped at a sample maximum burn-up of 58.9 MWd/kgHM, and then extended with zero power and cold conditions to the point of measurement for each nuclide, so that nuclide density data could be extracted for each isotope of interest at both end-of-life (EOL) and time of measurement. A similar approach was followed for the fuel assembly model, stopping at an assembly average burn-up that resulted in a sample burn-up of 58.9 MWd/kgHM. Burn-up step sizes of less than 1 MWd/kgHM were used in all depletion calculations, keeping the points in time at which the conditions changed according to the irradiation history, and accounting for the inter-cycle periods (zero power). In order to accurately compute the ^{135}Xe equilibrium concentration, initial burn-up steps were smaller than 1 MWd/kgHM, up to 5 MWd/kgHM.

4.5 Cases Analyzed

The depletion analysis for Sample BM5 was carried out by performing several separate sets of calculations in order to assess certain effects of the computational models. These included pin-cell vs. fuel-assembly treatment, J2LIB vs. ENDF/B-IV data library usage, as well as the effects of averaging irradiation history parameters and of fuel radial detail, (1 vs. 7 radial zones). All cases used the same number and length of depletion steps.

5. Results and Discussion

5.1 Base Cases

Table 1 compares calculated nuclide concentrations (*C*) and experimental measurements (*E*) in terms of *(C-E)/E %*. The calculations considered are for fuel-assembly (10 fuel zones in sample pin) and pin-cell (1 fuel zone) models using the J2LIB and ENDF/B-IV libraries, and experimental results from the PSI and SCK•CEN radio-chemical laboratories providing two independent sets of comparisons. The *2-*σ experimental errors are also included for assessment purposes. CASMO-4 predictions are, in general, in better agreement with the data from SCK•CEN for all cases analyzed. Different measurement techniques used by the two laboratories led to different accuracies in the data, reflected also in the comparison with CASMO-4 results.

5.1.1 Actinides

The nuclide densities of most of the major actinides, i.e. U, Pu, Np, Cm and Am, were calculated within ±10% of experimental values. In particular, an accurate $^{235}U/^{238}U$ ratio points to a good calculation of the burn-up, supported by small differences in the ratios $^{145}Nd/^{238}U$, $^{146}Nd/^{238}U$ and $^{148}Nd/^{238}U$, other common indicators of burn-up.

Regarding the Pu isotopes, the results for ^{238}Pu with J2LIB, particularly the SCK•CEN data, show larger differences than with ENDF/B-IV. A similar underestimation of ^{238}Pu in MOX fuel was observed by Roque et al. [5] using the DARWIN depletion environment and JEF2.2. The authors consequently suggested the revision of cross-section data for the reactions involved in ^{238}Pu build-up. ^{239}Pu, formed mainly by neutron capture in ^{238}U, is overpredicted by CASMO-4 following the methods and models reported in this paper. Apart from a posssibly too high neutron capture rate in ^{238}U, a too low ^{239}Pu neutron capture cross-section could also lead to the observed ^{239}Pu overprediction. The systematic underprediction of ^{240}Pu also supports a low $^{239}Pu(n,\gamma)^{240}Pu$ reaction rate. Regarding ^{241}Pu, for which self-shielding of the ^{240}Pu capture resonance at 1 eV is important, one can see how the use of the fuel-assembly model produces lower errors (see comparison with PSI results) than the simpler pin-cell model (1 fuel radial zone) with no resolution of the intra-assembly and intra-pin neutron flux (see Fig. 4 for the effect of a refined pellet radial description).

The content of ^{237}Np is significantly underpredicted by CASMO-4 and J2LIB. ^{237}Np is formed in MOX fuels mainly through the $^{238}U(n,2n)^{237}Np$ reaction, with a relatively small contribution from $^{235}U(n,\gamma)^{236}U \xrightarrow{\beta^-} {}^{237}Np$. The underestimation of $^{238}U(n,2n)^{237}Np$ reaction rates by JEF2.2, suggested in Ref.[5] based on the analysis of several experiments and fuel types, could explain the discrepancies observed and the better performance of ENDF/B-IV.

The ^{241}Am concentration is overestimated by CASMO-4 in all cases. This nuclide, mainly a result of ^{241}Pu decay, not influenced by depletion conditions, disappears through neutron capture to yield ^{242m}Am. The systematic underprediction of ^{242m}Am, appears to indicate that the calculated $^{241}Am(n,\gamma)^{242m}Am$ reaction rate is lower than expected. Roque et al. [5] observed errors of a similar magnitude with the DARWIN depletion package, and suggested the improvement of this reaction cross-section and of its reaction branching ratio in the epithermal region (it also yields ^{242}Am).

Good estimates of the concentration of ^{243}Cm and ^{245}Cm (close to within the experimental errors) are shown in Table 1 with J2LIB. The large error in the prediction of ^{242}Cm content, important as the only precursor of ^{243}Cm, could be explained in terms of a low ^{241}Am capture rate as mentioned above, ^{242}Am being its precursor through a short-lived (16 h) β^- decay.

Table 1 Comparison of CASMO-4 Calculated (*C*) with Experimental (*E*) Results for Sample BM5 Expressed as *(C-E)/E % (bold italics: less than exp. error ; italics: less than 10% difference)*

	PSI Measurements					SCK•CEN Measurements				
	Exp. Err	J2LIB (JEF2.2)		ENDF/B-IV		Exp. Err	J2LIB (JEF2.2)		ENDF/B-IV	
Nuclide	2σ	Fuel Ass.	Pin Cell	Fuel Ass.	Pin Cell	2σ	Fuel Ass.	Pin Cell	Fuel Ass.	Pin Cell
U-234	24.83	**-13.90**	**-13.06**	***-7.67***	***-6.76***	10.01	-16.58	-15.77	-10.13	*-9.25*
U-235	17.68	-21.36	-19.99	-24.40	-23.03	2.05	***-0.81***	***0.92***	*-4.66*	*-2.93*
U-236	10.67	***-6.35***	***-6.95***	***-7.04***	***-7.58***	5.02	*-6.53*	*-7.12*	*-7.38*	*-7.93*
U-238	4.18	***-0.28***	***-0.21***	***-0.37***	***-0.31***	0.45	***-0.28***	***-0.21***	***-0.37***	***-0.31***
Np-237	0.43	-16.68	-10.87	***0.42***	***0.09***	10.97	-20.76	-14.97	***-4.49***	***-4.81***
Pu-238	11.89	***-8.64***	***-7.88***	***4.15***	***5.10***	3.05	-20.77	-20.12	*-9.68*	*-8.86*
Pu-239	0.90	*9.41*	10.45	*8.42*	*9.53*	0.57	*3.27*	*4.25*	*2.33*	*3.38*
Pu-240	0.99	*-1.30*	*-3.41*	*-0.04*	*-2.22*	0.57	*-6.18*	*-8.19*	*-4.99*	*-7.06*
Pu-241	1.06	*3.69*	*6.67*	*3.30*	*6.21*	0.57	*-1.31*	*1.54*	*-1.69*	*1.08*
Pu-242	1.26	***-0.92***	***0.73***	*4.40*	*7.32*	0.57	*-4.96*	*-3.39*	***0.14***	*2.93*
Am-241	4.64	18.20	22.21	18.06	22.02	3.51	14.37	18.24	23.91	18.07
Am242m	5.33	-18.63	-14.15	-	-	10.59	-20.19	-15.80	-	-
Am-243	4.82	*8.47*	***-0.97***	-	21.64	3.51	*0.02*	*-4.42*	20.09	12.16
Cm-242	-	-	-	-	-	3.46	-79.97	-79.74	-79.38	-79.11
Cm-243	-	-	-	-	-	10.60	*-5.60*	*-5.93*	-10.36	-10.44
Cm-244	4.09	-14.49	-18.91	-14.23	-20.18	3.13	-11.43	-16.01	-11.16	-17.32
Cm-245	4.57	*-4.84*	*-9.25*	-11.27	-16.54	5.13	***-0.83***	*-5.42*	*-7.52*	-13.01
Gd-155	6.81	-39.07	-39.83	159.34	157.21	2.09	-26.72	-27.65	212.25	178.91
Eu-153	2.04	11.74	10.91	*7.27*	*6.68*	0.67	11.26	10.43	*6.81*	*6.22*
Eu-154	2.52	56.47	54.44	42.13	41.34	3.01	64.96	61.47	49.86	49.03
Eu-155	4.79	-29.14	-30.20	192.14	189.17	8.81	-35.02	-36.92	168.07	165.35
Ce-144	10.28	16.18	13.86	-	-	5.94	-55.86	-56.75	-	-
Nd-142	9.86	14.70	11.01	-	-	10.01	10.07	6.52	-	-
Nd-143	6.66	13.81	13.30	16.98	16.46	0.56	*5.05*	*4.58*	*7.98*	*7.51*
Nd-144	6.68	*7.44*	***5.85***	-	-	0.56	*1.71*	***0.17***	-	-
Nd-145	6.88	*7.62*	***6.74***	***1.45***	***0.71***	0.56	*3.40*	*2.55*	*-2.53*	*-3.24*
Nd-146	6.79	*7.12*	***5.69***	-	-	0.56	*5.22*	*3.81*	-	-
Nd-148	6.65	*7.50*	***6.33***	-	-	0.56	*6.33*	*5.17*	-	-
Nd-150	6.69	*7.45*	***6.30***	-	-	0.58	*4.83*	*3.71*	-	-
Pm-147	13.76	***7.11***	***6.47***	***-0.43***	***-0.88***	16.01	***-7.22***	***-7.78***	**-13.71**	**-14.11**
Sm-147	2.04	*-9.78*	*-9.54*	*-9.86*	*-9.63*	0.64	*-2.65*	*-2.42*	*-2.96*	*-2.74*
Sm-148	1.53	*-2.53*	*-3.77*	-	-	0.64	*4.30*	*2.98*	-	-
Sm-149	10.25	***-7.03***	***-5.70***	***-8.31***	***-6.72***	2.09	17.35	19.02	15.73	17.74
Sm-150	1.65	*-4.64*	*-5.79*	***0.20***	***-0.94***	0.64	*3.73*	*2.48*	*8.99*	*7.76*
Sm-151	2.28	19.84	20.59	16.78	18.04	0.79	32.78	34.36	29.73	31.13
Sm-152	1.89	*9.46*	*8.59*	*-5.66*	*-6.24*	0.64	21.92	20.96	*5.08*	*4.44*
Cs-133	2.99	*-3.68*	***-1.44***	***-1.59***	***-2.30***	3.06	***0.13***	***2.45***	***2.30***	***1.56***
Cs-134	3.41	17.70	14.90	20.91	17.98	3.09	22.15	19.24	24.75	21.72
Cs-135	2.85	***-0.91***	***1.86***	***2.06***	***2.20***	3.06	***1.95***	*4.80*	*5.01*	*5.14*
Cs-137	3.05	***-1.72***	***-2.82***	*3.28*	***2.15***	3.04	***2.20***	***1.06***	*7.40*	*6.22*
I-129	18.28	298.30	305.69	-	-	11.24	56.83	59.74	-	-
Sb-125	4.23	56.57	54.36	-	-	6.93	104.34	101.44	-	-
Ag-109	3.03	118.43	118.21	71.26	71.20	18.58	44.90	44.15	**13.14**	**13.09**
Ru-106	8.90	213.45	207.70	-	-	15.24	71.01	67.87	-	-
Ru-101	3.70	***-1.80***	***0.01***	-	-	16.13	40.60	43.20	-	-
Rh-103	4.23	-13.39	*-8.17*	-24.81	-25.07	9.93	50.45	59.51	30.61	30.15
Tc-99	2.09	*4.51*	*3.65*	-	-	19.47	**13.07**	**14.46**	-	-
Mo-95	4.86	*-10.19*	***-2.17***	-	-	9.70	***-6.50***	***1.85***	-	-
Sr-90	11.07	-11.45	-12.45	-	-	16.01	**12.13**	**11.02**	-	-

5.1.2 Fission Products

Regarding the important fission products Pm, Sm, and Cs, Table 1 shows that CASMO-4 can estimate their concentrations with an error less than or near ±10%, except for ^{134}Cs (~20%.) and ^{151}Sm (17 to 34%) and ^{152}Sm (~22% max.). ^{134}Cs is formed by neutron capture of ^{133}Cs and disappears also by neutron capture. The differences between the predictions of

^{133}Cs and ^{134}Cs seem to point to an underestimation of the ^{134}Cs capture rate. This cannot be conclusively stated, however, as the errors in the prediction of ^{135}Cs, the product of the ^{134}Cs (n,γ) reaction, are very small. Unfortunately, it is not possible to ascertain whether an overestimation of ^{151}Pm cumulative fission yields, its precursor, causes the excessive build-up of ^{151}Sm, since no data was available for ^{151}Pm. The ENDF/B-IV library seems to yield better predictions of the Sm vector.

The Nd vector is systematically overpredicted by the J2LB library, but, except for ^{142}Nd and ^{143}Nd, the calculation errors remain below 10%. Neodymium isotopes are produced in cascade by neutron capture from ^{142}Nd, which is formed by successive neutron captures and decays starting from ^{133}Cs and ending in ^{142}Pm (transformed into ^{142}Nd via β^- decay). A lack of specific experimental data, however, makes it difficult to ascertain which of the intermediate steps is causing the overestimation of ^{142}Nd, especially because the Cs isotopes are relatively well predicted. Thus, the larger calculated build-up of Nd isotopes could be related to larger capture rates of Ba, La, Ce or Pm isotopes.

The ^{154}Eu concentration is significantly overestimated, which is compatible with the large underestimation of ^{155}Eu, the capture product of ^{154}Eu. In fact, Ref.[5] suggests that modifications of the ^{154}Eu capture cross-section are needed in the JEF2.2 (J2LIB) library, since recent studies on ^{154}Eu and ^{155}Eu have shown that the cross-sections are not adequate and will be replaced by those compiled in ENDF/B-VI.7 for the new JEF3.0 library release. The ^{155}Eu underestimation affects the build-up of ^{155}Gd, its daughter through β^- decay, which, as a result, is clearly underpredicted by about the same magnitude with respect to both laboratories.

A clear overestimation of the ^{129}I concentration is seen with respect to the measurements reported by both laboratories. In the ARIANE report [2], the PSI measurement was discarded as not reliable, but, in general, the experimental procedure and the volatility of ^{129}I can lead to large uncertainties in the measurements that could explain the errors in Table 1, since CASMO-4 calculations maintain all the ^{129}I produced in the fuel sample without accounting for volatile losses.

The concentrations of some of the metallic nuclides are remarkably well predicted. Thus, the results for ^{99}Tc ^{95}Mo, ^{90}Sr and ^{101}Ru are within experimental uncertainties (only the PSI measurement being considered in the case of ^{101}Ru). Other important nuclides for burn-up credit calculations do not fare so well, however, with the results being somewhat better when compared to the SCK•CEN data. Large errors observed with respect to the PSI data suggest a less accurate measurement technique in general [2]. Nonetheless, the relatively large errors observed for certain metallic nuclides such as ^{106}Ru, ^{109}Ag, and ^{103}Rh, even for the SCK•CEN data, may be traced to the precipitation issue, also acknowledged in Ref.[5], where the authors reported errors of the same order of magnitude as those in the SCK•CEN comparisons and suggested that a better, more accurate program of dissolution could shed light on the reason for the discrepancies observed.

The analysis of Table 1 also leads to the conclusion that the use of a pin-cell model for the depletion calculations for Sample BM5 did not produce significantly less accurate results than accounting for the effects of the intra-assembly flux distribution with a fuel assembly model. In fact, for most isotopes, the results appear to be better with the pin-cell model. Only in the case of the Pu, Am and Cm vectors did the use of a more refined depletion model really lead to improvements. The build-up of these nuclides can be more accurately calculated when the neutron flux in the fuel region is described in greater detail. This outcome can also be seen in the context of the use of 7 radial zones in the pin-cell model (more accurate description of the intra-pin neutron flux), as discussed in Section 5.3.

5.2 Influence of Irradiation History

Figure 3 displays results for the detailed (base case) and averaged irradiation history modeling of the burn-up. Only the isotopes showing a significant effect are included. The variation in neutron spectrum brought about by changes in burn-up conditions is likely to result in changes in the build-up of nuclides. As expected, the averaging of the depletion conditions results in less accuracy for most nuclides, especially in the case of 6-cycle averaging. Figure 3 shows that for the major actinides, the use of a detailed depletion history yields, in general, more accurate results, especially in the build-up of ^{238}Pu. The largest effect of full averaging is an about 5% larger underprediction for ^{234}U. The predictions of ^{239}Pu, ^{242}Pu, and ^{241}Am seem to benefit, however, from the use of an average depletion history. The case of ^{241}Am and ^{242m}Am points to an increase in the ^{241}Am(n,γ)^{242m}Am reaction rate with respect to the detailed depletion history treatment that reduces the excess in ^{241}Am, increasing the amount of ^{242m}Am. The estimates ^{135}Cs and ^{137}Cs appear to improve when average conditions are used. *^{135}Cs*, a product of the decay of ^{135}Xe, and ^{137}Cs appears as a results of ^{137}Xe β^- decay (from neutron capture of ^{135}Xe and ^{136}Xe). Unfortunately, due to its short half-life (*hours*), no experimental data is available for ^{135}Xe to investigate this result further.

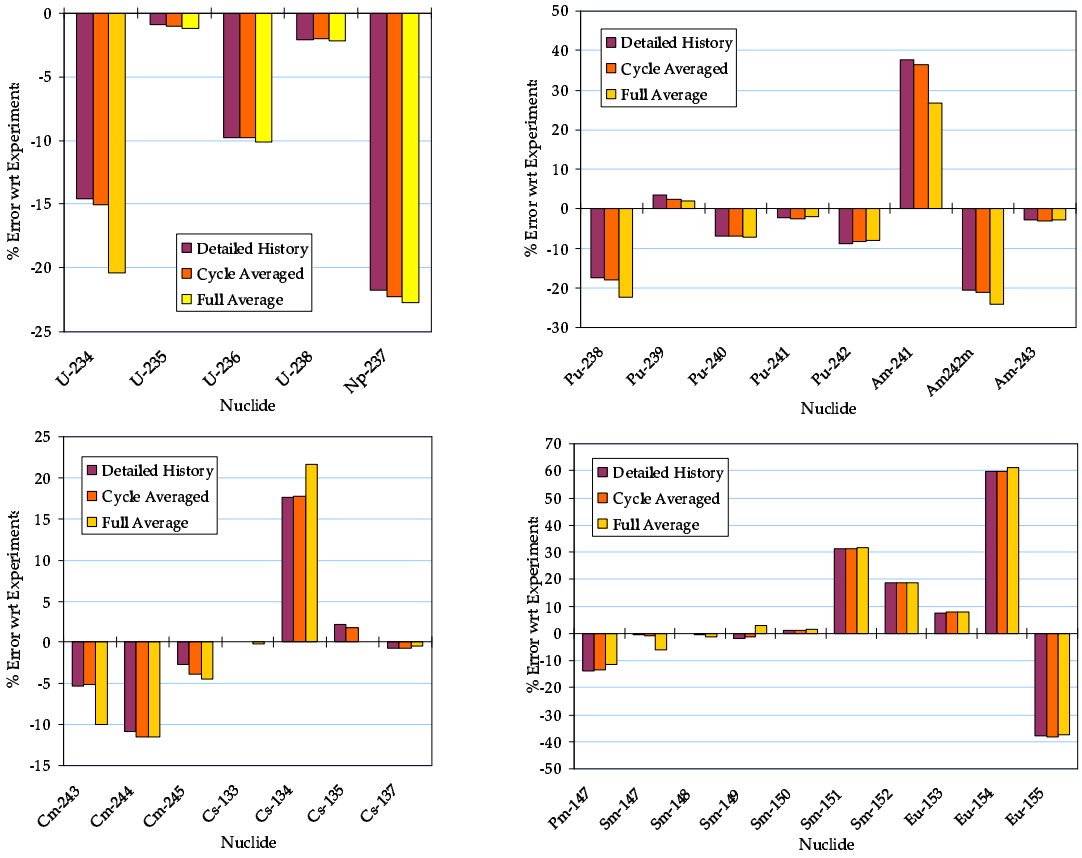

Fig. 3 Comparison of Results for Averaging of Irradiation History. Fuel-Assembly Model. *(EOL, J2LIB, SCK•CEN Measurements)*

5.3 Influence of Fuel Radial Description

The influence of a refined radial description of the fuel pellet on the isotopic build-up was studied by comparing the results of the pin-cell model at EOL employing 1 (base case) and 7

radial zones (see Fig. 2). Figure 4 shows these results for the nuclides whose build-up was most influenced by the more detailed fuel model. In the Pu vector, ^{240}Pu and ^{241}Pu predictions are seen to be improved, whereas the ^{242}Pu result appears to be worsened with the refined model. The Am vector is also significantly affected, especially ^{243}Am with differences in the results of more that 5%. In the case of Cm nuclides, only the estimates for ^{244}Cm and ^{245}Cm show about 3% improvement when the refined model is used. The effects of the increased radial resolution on the build-up of the rest of fission products and actinides are small, with variations of at most about ±1% with respect to the results obtained with a single radial zone. The metallic fission products were practically not affected. In general, the build-up of fission products, unless they have a large neutron absorption cross-section or are a product of another nuclide with a large (n,γ) cross-section, is not influenced by the intra-pellet neutron flux distribution. On the other hand, those nuclides with strong resonance capture cross-sections that lead to spatial self-shielding behavior, eg ^{240}Pu, ^{242}Pu, are likely to show a change in the prediction of their concentration with a more detailed description of the neutron flux inside the fuel pellet, as seen in Figure 4. This can provide better neutronic modeling for studying the so-called 'rim effect'.

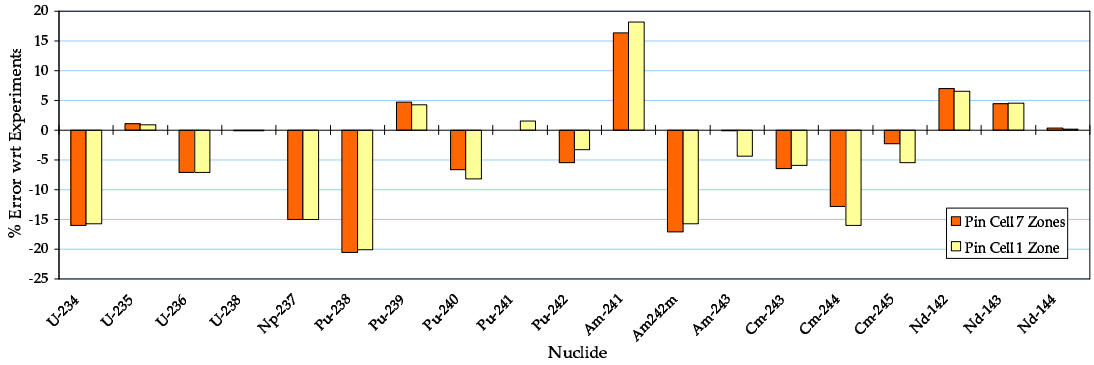

Fig. 4 Comparison of Results for Refined Fuel-Pellet Radial Model. Pin Cell Model. Detailed Burn-up History *(EOL, J2LIB, SCK•CEN Measurements)*

6. Conclusions

The most important conclusions to be drawn from this study are:

- Good predictions (error < 10%) of the important actinides, i.e. U, Pu, and Cm isotopes (except for ^{242}Cm) are possible for highly-burnt MOX fuel.
- Acceptable performance is obtained for the important fission products such as Cs (except for ^{134}Cs), Nd, Pm, and Sm (except for ^{151}Sm) with both libraries.
- Large discrepancies in the Eu vector, linked probably to inaccurate neutronic data in the two libraries [5], have a significant impact on the estimation of ^{155}Gd concentration.
- Some of the metallic nuclides, e.g. ^{99}Tc, ^{101}Ru, are accurately estimated. Discrepancies in others may be related to experimental difficulties in measuring metallic precipitates [2].
- The volatility of ^{129}I seems to have prevented both laboratories from a complete accounting, which could explain the large CASMO-4 overpredictions.
- The use of the J2LIB (JEF2.2) library produces in general better results than the ENDF/B-IV based library. Nuclide inventories of Pu isotopes, ^{237}Np and ^{234}U, however, are better estimated with ENDF/B-IV.
- A detailed depletion history description yields more accurate results for most isotopes, except for ^{241}Am, ^{239}Pu, ^{242}Pu, ^{135}Cs and ^{137}Cs, which seem to be more accurately

predicted with a 6-cycle average history.

- The pin-cell models with 1 and 7 fuel zones are seen to yield results of similar accuracy as, and in some cases better than, the more computing-intensive fuel assembly model, except for the Pu, Am and Cm vectors, where better intra-fuel assembly flux description yields more accurate results. As to be expected, refinement of the fuel radial description improves predictions for those nuclides which influence the so-called ‘rim effect’ (due to the improved self-shielding treatment). The differences in the accuracy for other nuclides are 1 to 2% at most, with the metallic fission products practically unaffected.

Acknowledgements

This work was partly funded by the Swiss Federal Nuclear Safety Inspectorate HSK (Hauptabteilung für die Sicherheit der Kernanlagen) and the Swiss Federal Office of Energy BFE (Bundesamt für Energie).

References

1) T. Aoust, "ARIANE Programme. Irradiation Data Report. Part 2", BN 9904537-AR 99/13 (1999).
2) D. Boulanger, M. Lippens, "Actinide Research in a Nuclear Element. Final Report", BN 0000253/221-B Report, BELGONUCLEAIRE (2000).
3) D. Knott, B.H. Forssén and M. Edenius, M., "CASMO-4. A Fuel Assembly Burn-up Program. Methodology", STUDSVIK/SOA-95/2 (1995).
4) J. Rhodes and M. Edenius, "CASMO-4. A Fuel Assembly Burn-up Program. User’s Manual", SSP-01/400 Rev.1(2001).
5) B. Roque, P. Thiollay, A. Marimbeau and A. Barreau, "Experimental Validation of the Code System „DARWIN“ for Spent Fuel Isotopic Predictions in Fuel Cycle Applications", Proc. of PHYSOR 2002, Seoul, Korea, October 7-10 (2002).